$B \to \mu^+\mu^-$ in the two-Higgs-doublet model

J. L. Hewett*
Ames Laboratory and Department of Physics, Iowa State University, Ames, Iowa 50011

S. Nandi
Department of Physics, Oklahoma State University, Stillwater, Oklahoma 74078

T. G. Rizzo
Ames Laboratory and Department of Physics, Iowa State University, Ames, Iowa 50011
(Received 23 May 1988)

The rare decay $B \to \mu^+\mu^-$ is studied within the context of the two-Higgs-doublet extension of the standard model. We show that for a reasonable range of model parameters, the charged-Higgs-scalar contribution exceeds the conventional contributions from the standard model. For the process $B_s \to \mu^+\mu^-$, branching fractions $\gtrsim 10^{-8}$ are possible in this scenario. For the process $Z \to b\bar{q} + \bar{b}q$, we find the charged-Higgs-boson contribution leads to branching fractions $\gtrsim 10^{-6}$.

The recent observation of B_d-$\bar{B}_d$ mixing by the ARGUS Collaboration[1] has revived interest in CP violation[2] and rare modes[3] in B-meson decays. In particular, there has been a significant amount of work examining the influence of non-standard-model physics [e.g., additional Higgs fields, a fourth generation of fermions, and supersymmetry (SUSY)][4] on rare B decays.

In this paper we wish to examine the influence of charged Higgs bosons, which result in the two-Higgs-doublet extension of the standard model (SM), on the rate decays $B_{d,s} \to \mu^+\mu^-$ and $Z \to b\bar{q} + \bar{b}q$. It has recently been pointed out that this simple extension can explain[5] the large B-$\bar{B}$ mixing without a heavy top quark, and also leads to much interesting phenomenology involving the light charged and possibly neutral Higgs bosons.[6] This two-Higgs-doublet extension is a common feature of many scenarios: SUSY, Peccei-Quinn models,[7] and E_6 superstring-inspired models.[8] In these two-Higgs-doublet models, each doublet gives a mass only to quarks of a given charge, thus avoiding difficulties associated with flavor-changing neutral-Higgs-boson exchange.[9] Each doublet obtains a vacuum expectation value (VEV) v_i ($i=1,2$) subject only to the constraint that $v_1^2+v_2^2=v^2$, with v being the usual VEV of the SM. One usually defines the quantity $\tan\beta=v_1/v_2$ so that generic charged-Higgs-boson coupling to the quarks is given by

$$\mathcal{L}=\frac{g}{2\sqrt{2}}\frac{1}{M_W}(\tan\beta)^{-1}\bar{u}_i V_{ij}(a_{ij}-b_{ij}\gamma_5)d_j H + \text{H.c.} , \quad (1)$$

with g being the usual $SU(2)_L$ coupling constant and V_{ij} being the relevant Kobayashi-Maskawa[10] matrix element. The coefficients a_{ij} and b_{ij} are given by

$$a_{ij} \equiv m_{u_i} + m_{d_j}\tan^2\beta, \quad b_{ij} \equiv m_{u_i} - m_{d_j}\tan^2\beta . \quad (2)$$

For leptons, assuming massless neutrinos, the corresponding couplings are

$$\mathcal{L}=\frac{g}{2\sqrt{2}}\frac{m_i}{M_W}(\tan\beta)\bar{\nu}_i(1+\gamma_5)l_i H + \text{H.c.} \quad (3)$$

Note that the $\bar{t}bH$ coupling grows rapidly with increasing m_t so that for some values of $\tan\beta$ it becomes strong. If we demand that this coupling not be *too* strong as to endanger perturbation theory one obtains a bound on $\tan\beta$ as a function of m_t. One signal for a large $\bar{t}bH$ coupling would be a "wide" t-quark, e.g., if $t \to bH$ is kinetically allowed we must demand $\Gamma_t/m_t \ll 1$. Similarly, if we demand that the $\bar{t}bH$ be smaller than, say, the QCD coupling ($\alpha_s \simeq 0.2$) a bound is obtained which is semiquantitatively similar. We will thus use the constraint

$$\tan\beta \ge \frac{m_t}{600\ \text{GeV}} \quad (4)$$

in our analysis that follows. The constraint (4) ensures a "narrow" t quark as well as a perturbative coupling at the $\bar{t}bH$ vertex.

The diagrams which may potentially contribute to the $B \to \mu^+\mu^-$ process are shown in Fig. 1. However, for on-shell muons in the final state, electromagnetic current conservation leads to a null contribution for the photon-exchange term. As we show in Appendix B, the box diagrams with HH, HW, and $H\phi$ (where ϕ is the unphysical Higgs field of the SM) exchange are all found to be chirally suppressed; i.e., they are scaled down by additional factors of m_μ/m_W in amplitude compared with those coming from the loop-generated $b\bar{q}Z$ vertex.

For completeness we calculate the general $\bar{q}bG$ vertex with G a gauge boson ($=\gamma$, Z, or gluon). We can take this vertex to be given by

$$ig\bar{q}(p)\Gamma_\lambda b(p+q)G^\lambda(q) . \quad (5)$$

Γ_λ can be decomposed in several ways. Two convenient decompositions are given by (neglecting the mass of the light quark q)

$$\Gamma_\lambda = D\gamma_\lambda(1-\gamma_5)+Ep_\lambda(1+\gamma_5)+Fq_\lambda(1+\gamma_5) \tag{6}$$

and (with m_0 being the b-quark mass)

$$\Gamma_\lambda=(D+\tfrac{1}{2}m_bE)\gamma_\lambda(1-\gamma_5) \\ +(F-\tfrac{1}{2}E)q_\lambda(1+\gamma_5) \\ +i\frac{E}{2}\sigma_{\lambda\nu}q^\nu(1+\gamma_5) \tag{7}$$

which can be obtained from (6) by using the Gordon decomposition. We obtain the following expressions for the factors D, E, and F:

$$D=\frac{G_F m_t^2}{8\sqrt{2}\,\pi^2}(V_{tb}V_{tq}^*)(\tan^2\beta)^{-1}\sum_{i=1}^{3}D_i\ ,$$
$$E=-\frac{G_F m_b}{4\sqrt{2}\,\pi^2}(V_{tb}V_{tq}^*)\sum_{i=1}^{2}E_i\ , \tag{8}$$
$$F=-\frac{G_F m_b}{4\sqrt{2}\,\pi^2}(V_{tb}V_{tq}^*)\sum_{i=1}^{2}F_i\ ,$$

where the sum extends over the various contributing diagrams in Fig. 1.

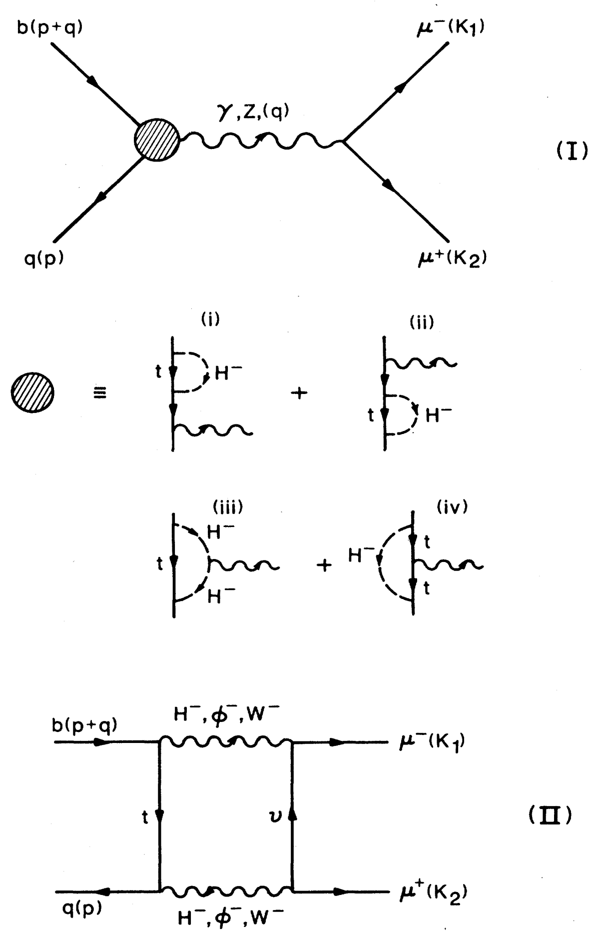

FIG. 1. Diagrams contributing to the process $B\to\mu^+\mu^-$.

Terms labeled with the index 1 originate from diagram (iii) where the gauge boson attaches itself to the H^-; terms labeled with the index 2 come from diagram (iv) where the gauge boson couples to the t quark; terms labeled with the index 3 arise from the self-energy diagrams (i) and (ii). Explicitly we have

$$D_1=CJ_{11}\ ,$$
$$D_2=C'[(V+A)J_9-(V-A)J_{10}]\ ,$$
$$D_3=C'(V'+A')J_{12}\ ,$$
$$E_1=C[J_1+J_2(\tan^2\beta)^{-1}]\ , \tag{9}$$
$$E_2=C'[(V+A)J_5+(V-A)J_6 \\ +(V-A)J_7(\tan^2\beta)^{-1}]\ ,$$
$$F_1=C[J_3+J_4(\tan^2\beta)^{-1}]\ ,$$
$$F_2=C'[(V-A)J_6+(V-A)J_8(\tan^2\beta)^{-1}]\ .$$

In (9) the coefficients C, C', V, V', A, and A' are given in Table I for $G=\gamma$, Z, and g. J_i $(i=1,12)$ are integrals over Feynman parameters which we evaluate numerically and are given in Appendex A. Given Eqs. (5)–(9) and the integrals in Appendix A, we have complete expressions for the general $\bar{q}bG$ vertex resulting from charged-Higgs-scalar exchange.[11]

A short calculation shows that the $q\bar{b}G$ amplitude is finite. The poles from each diagram can be summed and lead to a term proportional to

$$-C'(V'+A')+C'(V-A)-C \tag{10}$$

which vanishes for each of $G=\gamma$, Z, or g.

To proceed with the $B\to\mu^+\mu^-$ calculation, we couple the off-shell Z boson to a pair of muons and obtain the desired amplitude (in the $q^2=m_B^2\to 0$ limit)

$$-ig^2C_Z'M_Z^{-2}\bar{q}(p)\Gamma_\lambda^Z b(p+q)\bar{\mu}(k_1)\gamma^\lambda(v_\mu-a_\mu\gamma_5)\mu(k_2)\ , \tag{11}$$

where

$$v_\mu=\frac{1}{2c_W}\left[-\frac{1}{2}+2x_W\right]\ ,$$
$$a_\mu=\frac{1}{2c_W}\left[-\frac{1}{2}\right]\ , \tag{12}$$
$$c_W=\cos\theta_W\ .$$

Using standard current-algebra relations and neglecting terms of order m_q, we obtain the following decay rate for $B\to\mu^+\mu^-$:

$$\Gamma=\frac{G_F^2 m_B^5}{2\pi}\left[\frac{f_{Bq}^2}{m_{Bq}^2}\right]\left[\frac{m_\mu^2}{m_{Bq}^2}\right]\left[1-4\frac{m_\mu^2}{m_{Bq}^2}\right]^{1/2}(2c_WX)^2 \tag{13}$$

with m_{B_q} (f_{B_q}) being the mass (decay constant) of the B meson and

TABLE I. Couplings and coefficients used in obtaining the $b\bar{q}G$ amplitude. T_i are the $SU(3)_c$ generators.

Gauge boson	C	C'	V	A	V'	A'
γ	$-\sin\theta_W$	$\sin\theta_W$	$\frac{2}{3}$	0	$-\frac{1}{3}$	0
Z	$\frac{\cos 2\theta_W}{2\cos\theta_W}$	$\frac{1}{2\cos\theta_W}$	$\frac{1}{2}-\frac{4}{3}x_W$	$\frac{1}{2}$	$-\frac{1}{2}+\frac{2}{3}x_W$	$-\frac{1}{2}$
g	0	g_s/g	T_i	0	T_i	0

$$X \equiv (D+\tfrac{1}{2}m_bE)+\frac{m_{Bq}^2}{m_b}(F-\tfrac{1}{2}E) . \tag{14}$$

To be specific we consider the decay $B_s \to \mu^+\mu^-$; the corresponding decay rate for $B_d \to \mu^+\mu^-$ is obtained by an approximate rescaling (assuming $f_{B_d} \simeq f_{B_s}$ and $m_{B_d} \simeq m_{B_s}$)

$$\Gamma(B_d \to \mu^+\mu^-) = \frac{|V_{td}^*|^2}{|V_{ts}^*|^2}\Gamma(B_s \to \mu^+\mu^-) . \tag{15}$$

In our numerical calculations we take $f_{B_s}=100$ MeV (corresponding to $f_\pi=93.3$ MeV), $m_{B_s}=m_{B_d}$, and $|V_{tb}V_{ts}^*|=|(0.98)(0.042)|$. Other choices of these parameters lead to different values of Γ_d which can be obtained by simple rescaling.

Figures 2–5 show the branching fraction for $B_s \to \mu^+\mu^-$ from the charged-Higgs-boson contribution to the amplitude only, for four values of the t-quark mass ($m_t=50$, 100, 150, and 200 GeV, respectively) as a function of the charged-Higgs-scalar mass (m_H) for different values of $\tan\beta$ consistent with the constraint on the Higgs-boson coupling in Eq. (4). Also shown in each figure is the prediction of the SM for the same t-quark masses as given above as obtained from the work of Inami and Lim.[12] Note that in all cases the branching

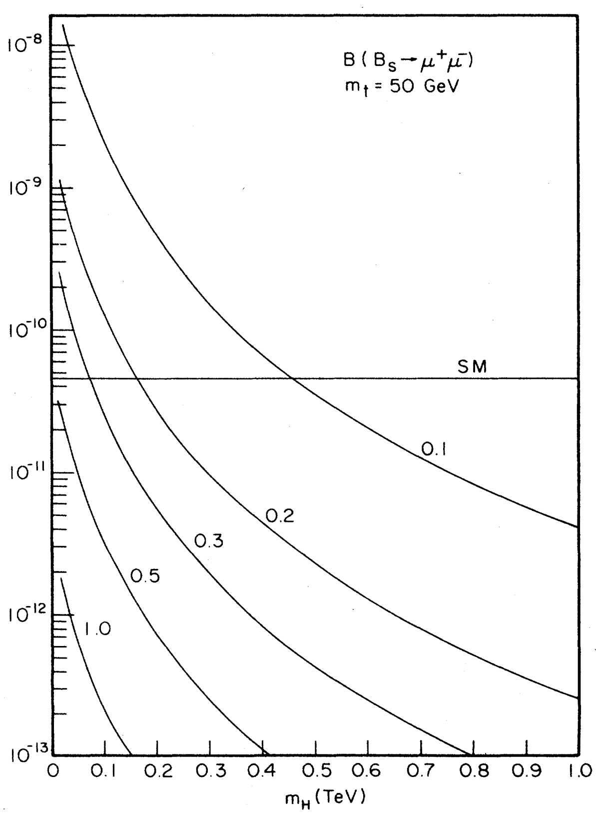

FIG. 2. The branching fraction for $B_s \to \mu^+\mu^-$ as a function of m_H with $m_t=50$ GeV for different values of $\tan\beta$ consistent with our constraint on the $\bar{t}bH$ coupling. Also shown is the SM prediction.

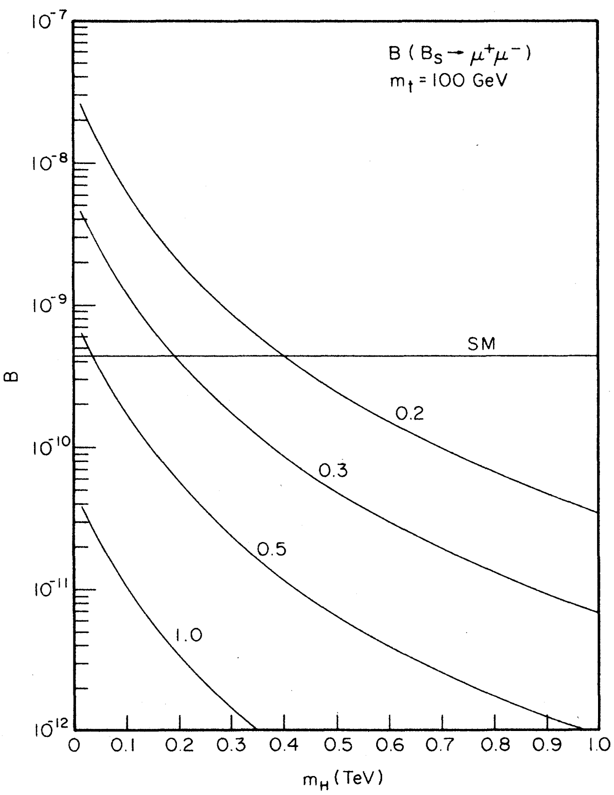

FIG. 3. Same as Fig. 2 but for $m_t=100$ GeV.

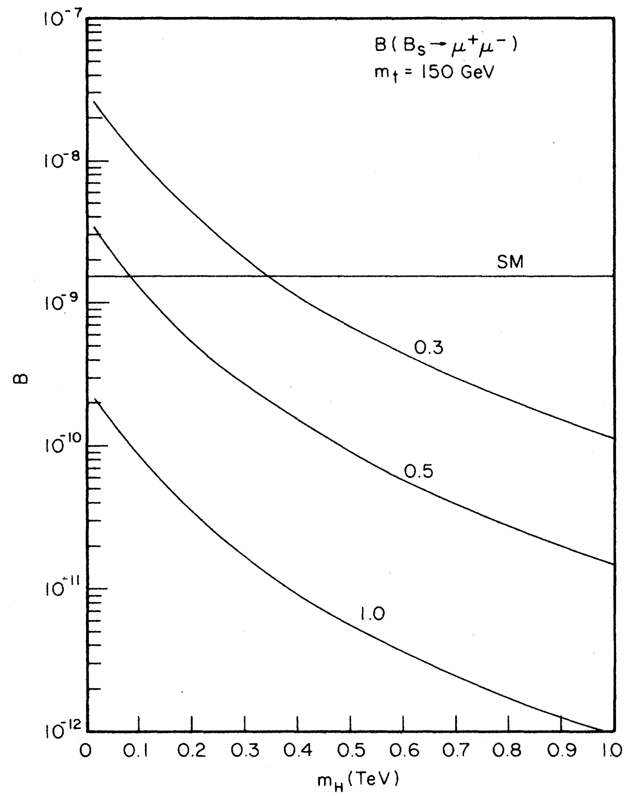

FIG. 4. Same as Fig. 2 but for $m_t = 150$ GeV.

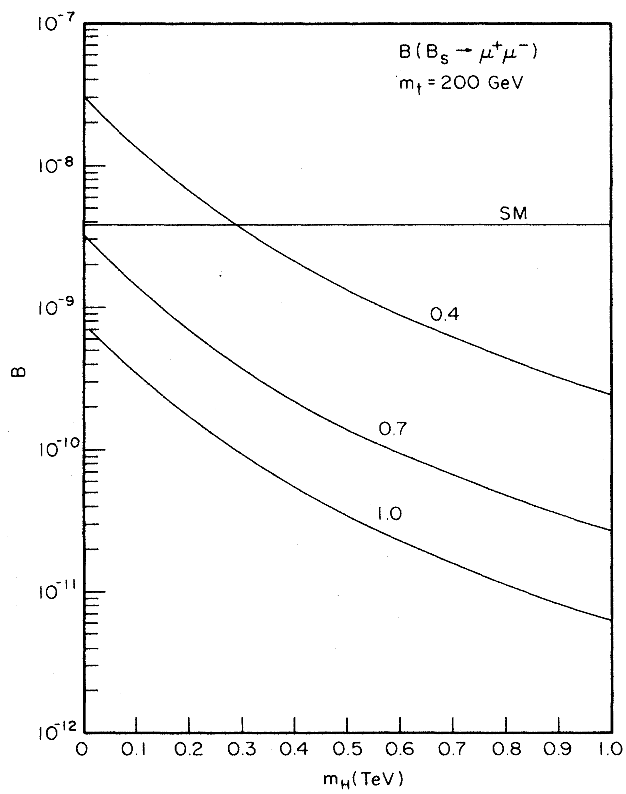

FIG. 5. Same as Fig. 2 but for $m_t = 200$ GeV.

fraction B falls quite rapidly with both increasing m_H and $\tan\beta$. For $m_t = 50$ GeV (where small $\tan\beta$ values are allowed by our coupling constraint) there is a significant region of parameter space which leads to values of B which are much larger than that predicted by the SM. For example, if $m_H = 200$ GeV and $\tan\beta = 0.1$, the charged-Higgs-boson contribution to the branching fraction exceeds that from the SM by an order of magnitude. As m_t increased (see Fig. 3), the SM prediction for B increases whereas $\tan\beta$ is now further constrained by Eq. (4). This leads to a more restricted parameter space than in the $m_t = 50$ GeV case where the charged-Higgs-boson contribution can be significantly larger than that from the SM. Note also that for fixed $\tan\beta$ as m_t is increased the curves for B as a function of m_H flatten out with increasing m_H. These trends continue in the cases of $m_t = 150$ and 200 GeV as shown in Figs. 4 and 5, respectively, where the coupling constraint [Eq. (4)] is even stronger. Once $m_t = 200$ GeV is reached, there is only a rather small region of parameter space which leads to B values larger than that predicted by the SM. Even in this small region, the increase in B is at most a factor of 7–8 over its SM value. It is thus clear from this analysis that due to the coupling constraint, charged-Higgs-boson effects will be most noticable if m_t is small ($\simeq 50$ GeV) and $\tan\beta$ takes on small values ($\lesssim 0.25$) as well.

What are the prospects for observing decays such as $B_s \to \mu^+\mu^-$ at branching fractions of order 10^{-8}? The prospect of searching for rare B decays at the Superconducting Super Collider (SSC) has been a subject of much discussion in the past few years and spectrometers especially suited for this kind of physics have been designed.[13] While the rate for $b\bar{b}$ production at the SSC is very high ($\sim 5 \times 10^5$ pairs/sec at a luminosity of 10^{33} $\mathrm{cm}^{-2}\mathrm{sec}^{-1}$) not all b's which are produced can be used to study rare decays. Cox and Wagoner,[13] using the $B \to J/\psi + X$ trigger to unambiguously tag b's (including trigger efficiencies and detector acceptances) estimate that $\sim 6 \times 10^8$ B_s mesons will be usable (per 10^7-sec year) to study rare B_s modes. This estimate includes a factor of $\sim \frac{1}{5}$ for $b \to B_s$ and assumes a 12-GeV muon absorber. The $B_s \to \mu^+\mu^-$ mode will be easily reconstructed with high efficiency in such a detector and usable rates are sufficiently large to explore the range of branching fractions discussed here ($\sim 10^{-8}$).

This same mode should also be observable at dedicated B factories using e^+e^- collisions.[14] While backgrounds are somewhat smaller for e^+e^- machines, B_s production rates are also smaller. One should not expect more than 10^6–10^7 B_s's/yr at such machines making it difficult if not impossible to explore branching fractions as small as $\sim 10^8$. Thus it seems that the SSC offers the best prospect for seeing the $B_s \to \mu^+\mu^-$ decay mode.

How about the rare Z decay modes ($b\bar{q} + \bar{b}q$) induced by charged Higgs scalars? Using Eqs. (5)–(9) and noting that F terms do not contribute here (since $q \cdot \epsilon_Z = 0$) we find that

$$\Gamma(Z \to b\bar{q} + \bar{b}q) = \frac{g^2 M_Z}{\pi}\left(D^2 + \tfrac{1}{8} M_Z^2 E^2\right) \tag{16}$$

TABLE II. Values of the branching fraction (B) for $Z\rightarrow b\bar{q}+\bar{b}q$ arising from charged-Higgs-boson-exchange loop diagrams for different values of m_t and m_H. In each case the value of $\tan\beta$ was chosen to maximize the value of B consistent with our constraint on the charged-Higgs-boson coupling to the t quark.

M_t (GeV)	M_H (GeV)	$\tan\beta$	B_Z
50	50	0.1	1.72×10^{-7}
50	200	0.1	6.31×10^{-7}
50	500	0.1	7.37×10^{-7}
50	1000	0.1	7.66×10^{-7}
100	50	0.2	6.45×10^{-8}
100	200	0.2	6.49×10^{-7}
100	500	0.2	7.56×10^{-7}
100	1000	0.2	7.75×10^{-7}
150	50	0.3	9.03×10^{-11}
150	200	0.3	5.69×10^{-7}
150	500	0.3	7.49×10^{-7}
150	1000	0.3	7.77×10^{-7}
200	50	0.4	4.51×10^{-8}
200	200	0.4	4.66×10^{-7}
200	500	0.4	7.27×10^{-7}
200	1000	0.4	7.75×10^{-7}

which can be compared to the more typical decay mode $Z\rightarrow\nu\bar{\nu}$:

$$\Gamma(Z\rightarrow\nu\bar{\nu})=\frac{g^2M_Z}{96\pi c_W^2}\ . \tag{17}$$

Table II shows the values of $B_Z=\Gamma(Z\rightarrow b\bar{q}+\bar{b}q)/\Gamma(Z\rightarrow\text{all})$ with $q=s$ for representative values of m_t and M_H with $\tan\beta$ chosen in each case so as to maximize this ratio. One sees that in all the cases shown the value of $B_Z\lesssim7.8\times10^{-7}$; the largest value we found ($B_Z=1.2\times10^{-6}$) was for $m_t=175$ GeV, $m_H=25$ GeV, and $\tan\beta=0.3$. The ratio is very small due to small Kobayashi-Maskawa (KM) angle factors as well as the coupling constraint [Eq. (4)]. For $q=d$ final states B_Z will be even smaller by the ratio of $|V_{td}|^2/|V_{ts}|^2$. Since $B_Z\lesssim10^{-6}$ it is clear that this mode will be unobservable at upcoming CERN LEP I and SLAC Linear Collider (SLC) experiments.

In conclusion we have examined the influence of charged-Higgs-scalar exchange on the rare processes $B\rightarrow\mu^+\mu^-$ and $Z\rightarrow b\bar{q}+\bar{q}q$. In the former case we found that branching fractions for $B_s\rightarrow\mu^+\mu^-$ can be larger than 2×10^{-8} (for our values of the KM elements and f_{B_s}) while the similar branching fraction for $B_d\rightarrow\mu^+\mu^-$ will be scaled down by a factor $|V_{td}|^2/|V_{ts}|^2$. The present experimental limit for $B_d\rightarrow\mu^+\mu^-$ is $\leq5\times10^{-5}$ (Ref. 15). The region of low m_t and small $\tan\beta$ produces the largest enhancement of these rate decays due to a charged Higgs scalar. The rare process $Z\rightarrow b\bar{q}+\bar{b}q$ has a very small branching fraction ($\sim10^{-7}$) in the model discussed here.

Finally, let us mention that we have been rather conservative to choose the allowed values of $\tan\beta$ by using the constraint given in Eq. (4). The ratio of the vacuum expectation values (VEV's) of the two Higgs-boson doublets, v_2/v_1 ($\equiv1/\tan\beta$) is a very important parameter in this calculation, since the dominant term, D in Eqs. (8) and (14), depends on the fourth power of this ratio. For example, choosing $(v_2/v_1)=10$ and $m_t=100$ GeV, we get the values of the branching ratio, $B(B_s\rightarrow\mu^+\mu^-)=(3,\ 2,\ 1)\times10^{-7}$ for $m_H=(25,\ 50,\ 100)$ GeV, respectively. This choice would correspond to $f_{t\bar{b}H}^2/4\pi\simeq0.6$. Similarly, for the same ratio of the VEV's, but $m_t=75$ GeV, we get $B=(1,\ 0.5)\times10^{-7}$ for $m_H=(25,\ 50)$ GeV, respectively. This choice corresponds to $f_{t\bar{b}H}^2/4\pi\simeq0.4$. For such choices, the branching ratio for the process $Z\rightarrow b\bar{q}+\bar{b}q$ is also enhanced significantly. Thus, larger values of the branching ratios are possible than those given in Figs. 2–5 and Table II.

J.L.H. and T.G.R. would like to thank the Physics Department of Oklahoma State University, where part of this work was done, for its hospitality. The work of J.L.H. was supported by the American Association of University of Women and by ZONTA International. This research was supported in part by the U.S. Department of Energy, Contract No. W-7405-82, Office of Energy Research (KA-01-01), Division of High Energy and Nuclear Physics (T.G.R.), and the U.S. Department of Energy Grant No. DE/FG05/85ER40215 (S.N.). S.N. also acknowledges the research support from a Dean's Incentive Grant from the College of Arts and Sciences of the Oklahoma State University.

APPENDIX A

In this appendix we give the explicit expressions for the integrals used in the text with $\delta\equiv m_t^2/m_H^2$ and $\epsilon\equiv-q^2/m_H^2$:

$$J_1=\delta\int_0^1 dx\int_0^{1-x}dy\, D_1^{-1}(1-x-y) \underset{q^2\to 0}{=} \delta\int_0^1 \frac{t(1-t)dt}{t+\delta(1-t)}\ , \tag{A1}$$

$$J_2=\delta\int_0^1 dx\int_0^{1-x}dy\, D_1^{-1}y(1-x-y) \underset{q^2\to 0}{=} \frac{\delta}{2}\int_0^1 \frac{t^2(1-t)dt}{t+\delta(1-t)}\ , \tag{A2}$$

$$J_3=\delta\int_0^1 dx\int_0^{1-x}dy\, D_1^{-1}\tfrac{1}{2}(1-2y) \underset{q^2\to 0}{=} \frac{\delta}{2}\int_0^1 \frac{t(1-t)dt}{t+\delta(1-t)}=\frac{1}{2}J_1\ , \tag{A3}$$

$$J_4=\delta\int_0^1 dx\int_0^{1-x}dy\, D_1^{-1}\tfrac{1}{2}y(1-2y) \underset{q^2\to 0}{=} \delta\int_0^1 \frac{\frac{1}{4}t^2-\frac{1}{3}t^3}{t+\delta(1-t)}dt\ , \tag{A4}$$

where $D_1\equiv\epsilon xy+(x+y)+\delta(1-x-y)$. Similarly, we obtain

$$J_5=\delta\int_0^1 dx\int_0^{1-x}dy\, D_2^{-1}y \underset{q^2\to 0}{=} \tfrac{1}{2}\delta\int_0^1 \frac{(1-t)^2dt}{t+\delta(1-t)}\ , \tag{A5}$$

$$J_6=\delta\int_0^1 dx\int_0^{1-x}dy\, D_2^{-1}(1-x-y) \underset{q^2\to 0}{=} \tfrac{1}{2}\delta\int_0^1 \frac{(1-t)^2dt}{t+\delta(1-t)}=J_5\ , \tag{A6}$$

$$J_7=\delta\int_0^1 dx\int_0^{1-x}dy\, D_2^{-1}x(1-x-y) \underset{q^2\to 0}{=} \tfrac{1}{2}\delta\int_0^1 \frac{t(1-t)^2dt}{t+\delta(1-t)}\ , \tag{A7}$$

$$J_8=\delta\int_0^1 dx\int_0^{1-x}dy\, D_2^{-1}(x+y)(1-x-y) \underset{q^2\to 0}{=} \tfrac{1}{6}\delta\int_0^1 \frac{(1+2t)(1-t)^2dt}{t+\delta(1-t)}\ , \tag{A8}$$

$$J_9=\delta\int_0^1 dx\int_0^{1-x}dy(-D_2^{-1}) \underset{q^2\to 0}{=} -\delta\int_0^1 \frac{(1-t)dt}{t+\delta(1-t)}\ , \tag{A9}$$

$$J_{10}=\int_0^1 dx\int_0^{1-x}dy[\epsilon(1-x-y)yD_2^{-1}+1+\ln D_2] \underset{q^2\to 0}{=} \tfrac{1}{2}+\int_0^1 dt(1-t)\ln[t+\delta(1-t)]\ , \tag{A10}$$

where $D_2\equiv x+\delta(1-x)-\epsilon(y^2-y+xy)$. Also, we obtain

$$J_{11}=\int_0^1 dx\int_0^{1-x}dy\,\ln D_1 \underset{q^2\to 0}{=} \int_0^1 dt\, t\ln[t+\delta(1-t)]\ , \tag{A11}$$

$$J_{12}=\int_0^1 dt(1-t)\ln(1-t+\delta t)\ . \tag{A12}$$

Note that the $q^2=m_B^2\to 0$ limit is appropriate for the $B\to\mu^+\mu^-$ process, whereas for $Z\to b\bar{q}+\bar{b}q$, $q^2=m_Z^2$ and is not negligible.

APPENDIX B

In this appendix we give the expression for the chirally suppressed amplitudes contributing to the $B\to\mu^+\mu^-$ process arising from the various box diagrams (*HH*, *WH*, and *ϕH*) shown in Fig. 1. In what follows we define $x_i\equiv m_i^2/M_W^2$.

We find the following contributions.

HH:

$$i\frac{G_F^2M_W^2}{32\pi^2}(V_{tb}V_{tq}^*)x_tx_\mu H_1\bar{q}\gamma_\lambda(1-\gamma_5)b\bar{\mu}\gamma^\lambda(1-\gamma_5)\mu\ , \tag{B1}$$

with

$$H_1\equiv-(x_t-x_H)^{-1}-x_t(x_t-x_H)^{-2}\ln(x_t/x_H)\ . \tag{B2}$$

ϕH:

$$2i\frac{G_F^2M_W^2}{32\pi^2}(V_{tb}V_{tq}^*)x_tx_\mu H_2\bar{q}\gamma_\lambda(1-\gamma_s)b\bar{\mu}\gamma^\lambda(1-\gamma_5)\mu\ , \tag{B3}$$

where

$$H_2\equiv\frac{x_H\ln x_H-x_t\ln x_t+x_tx_H\ln(x_t/x_H)}{(1-x_H)(1-x_t)(x_H-x_t)}\ . \tag{B4}$$

WH:

$$i\frac{G_F^2M_W^2}{32\pi^2}(V_{tb}V_{tq}^*)(x_bx_\mu)^{1/2}(\tan^2\beta)H_2\bar{q}\gamma_\lambda(1-\gamma_5)\times\gamma_\alpha b\bar{\mu}\gamma^\alpha\gamma^\lambda(1-\gamma_5)\mu\ . \tag{B5}$$

One sees that in all cases, chiral suppression exists in each of the above terms. Both *HH* and *ϕH* terms $\sim x_\mu$ whereas the *WH* term $\sim(x_\mu x_b)^{1/2}$ and is further suppressed by $\tan^2\beta$ (assuming $\tan^2\beta<1$, of course).

---

*Present address: Physics Department, University of Wisconsin, Madison, WI 53706.

[1]ARGUS Collaboration, H. Albrecht *et al.*, Phys. Lett. B **192**, 245 (1987).

[2]I. I. Bigi and A. I. Sanda, Phys. Lett. B **194**, 307 (1987); M. Lusignoli, CERN Report No. CERN-TH-4977/88, 1988 (unpublished). For recent reviews, see also M. K. Gaillard, talk presented at *B*-Meson Factory Workshop, SLAC, 1987 (unpublished); F. J. Gilman, in *Proceedings of the International Symposium on the Production and Decay of Heavy Flavors*, Stanford, California, 1987, edited by E. D. Bloom and A. Friedman (World Scientific, Singapore, in press).

[3]For recent reviews see A. Soni, talk presented at *B*-Meson Factory Workshop, SLAC, 1987 (unpublished); N. G. Deshpande and J. Trampetić, in *Proceedings of the International Symposium on the Production and Decay of Heavy Flavors* (Ref. 2); see also Gaillard (Ref. 2) and Gilman (Ref. 2).

[4]S. Bertolini, F. Borzumati, and A. Masiero, Nucl. Phys. **B294**,

321 (1987); T. G. Rizzo, Phys. Rev. D **38**, 820 (1988); B. Grinstein and M. B. Wise, Phys. Lett. B **210**, 274 (1988); R. M. Godbole, U. Türke, and M. Wirbel, *ibid.* **194**, 302 (1987); J. L. Hewett, *ibid.* **193**, 327 (1987); G. Eilam, J. L. Hewett, and T G. Rizzo, Phys. Rev. D **34**, 2773 (1986); A. Soni, in Proceedings of the First International Symposium on the Fourth Family of Quarks and Leptons, Santa Monica, California, 1987, edited by D. Cline and A. Soni (to be published).

[5]S. L. Glashow and E. E. Jenkins, Phys. Lett. B **196**, 233 (1987).

[6]S. Nandi, Phys. Lett. B **202**, 385 (1988); V. Barger and K. Whisnant, University of Wisconsin/Iowa State Report No. MAD/PH/401, 1988 (unpublished).

[7]H. E. Haber and G. L. Kane, Phys. Rep. **117**, 75 (1985); R. D. Peccei and H. R. Quinn, Phys. Rev. D **16**, 1791 (1977); Phys. Rev. Lett. **38**, 1440 (1977); S. Weinberg *ibid.* **40**, 223 (1978); F. Wilczek, *ibid.* **40**, 279 (1978).

[8]For a recent review of E_6 phenomenology see J. L. Hewett and T. G. Rizzo, Phys. Rep. (to be published).

[9]S. Glashow and S. Weinberg, Phys. Rev. D **15**, 1958 (1977); E. A. Paschos, *ibid.* **15**, 1966 (1977).

[10]M. Kobayashi and T. Maskawa, Prog. Theor. Phys. **49**, 673 (1973).

[11]A partial calculation of this vertex is given by W. S. Hou and R. S. Willey, Phys. Lett. B **202**, 591 (1988).

[12]T. Inami and C. S. Lim, Prog. Theor. Phys. **65**, 297 (1981).

[13]See, for example, B. Cox, F. J. Gilman, and T. Gottschalk, in *Physics of the Superconducting Super Collider,* proceedings of the Summer Study, Snowmass, Colorado, 1986, edited by R. Donaldson and J. Marx (Division of Particles and Fields of the APS, New York, 1987), p. 33; B. Cox and D. E. Wagoner, *ibid.*, p. 83; N. G. Deshpande and A. Soni, *ibid.*, p. 58; K. J. Foley *et al.*, in *Experiments, Detectors, and Experimental Areas for the Supercollider,* proceedings of the Workshop, Berkely, California, 1987, edited by R. Donaldson and M. G. D. Gilchriese (World Scientific, Singapore, 1988), pp. 701 and 759.

[14]See, for example, E. Bloom, in *Proceedings of the 1987 Vanderbilt Conference, Collider Physics: Current Status and Future Prospects,* Nashville, Tennessee, 1987, edited by J. E. Brau and R. S. Panvini (World Scientific, Singapore, 1988), p. 307.

[15]ARGUS Collaboration, H. Albrecht *et al.*, Phys. Lett. B **199**, 451 (1987).